

Box Decoding with Low-Complexity Sort-free Candidate Pruning for MIMO Detection

Shengchun Yang, Amit Sravan Bora, Member, IEEE, Emil Matus and Gerhard Fettweis, Fellow, IEEE

Abstract—Box Decoding is a sort-free tree-search MIMO detector whose complexity does not scale with the QAM order, achieved by searching a fixed candidate “box” around a zero-forcing (ZF) estimate. Prior work primarily reports small dimensions (e.g. 2×2), since the search visits an exponentially growing number of nodes as the MIMO order increases when no pruning is applied. This letter introduces three deterministic pruning rules that exploit QAM-grid symmetry and relative displacement between the ZF estimate and the nearby QAM points to eliminate unlikely branches, avoiding metric sorting and reducing full metric distance calculations. Simulations show large complexity savings with only a small impact on error performance. The resulting detector preserves QAM-order independence, scales to larger MIMO sizes, and maps naturally to parallel hardware implementation.

Index Terms—MIMO detection, Box Decoding, Low-complexity, \mathbf{K} -Best algorithm, Sort-free, Large-scale MIMO.

I. Introduction

MIMO detection has been studied in communication systems, yet the performance–complexity trade-off is difficult to manage when systems scale to large antenna dimensions in 5G and beyond [1], [2]. Optimal nonlinear detectors such as maximum likelihood (ML) and maximum a posteriori (MAP) provide the best error-rate performance, but their computational cost grows exponentially with modulation order and MIMO dimension [2]. Linear receivers, including Zero Forcing (ZF) and linear minimum mean square error (LMMSE), sit at the opposite: they are attractive for hardware implementation due to their simple processing flow, but with substantial performance loss, particularly in ill-conditioned channels [2].

To bridge this gap, near-ML tree-search detectors have been widely investigated. Depth-first sphere decoding (SD) [3] and breadth-first K-Best search [4] offer practical trade-off between complexity and performance. However, real implementations are often constrained by the candidate-selection stage. In many K-Best realizations, selecting the surviving paths requires sorting, which is inherently hardware-unfriendly, involving wide comparator networks and deep critical paths that scale poorly with both K and the constellation size $|\mathcal{A}|$ [5], [6].

The authors are with the Vodafone Chair for Mobile Communications Systems, Technische Universität Dresden, 01062 Dresden, Germany (e-mail: shengchun.yang@tu-dresden.de; amit.bora@tu-dresden.de; emil.matus@tu-dresden.de; gerhard.fettweis@tu-dresden.de).

This work has been submitted to the IEEE for possible publication. Copyright may be transferred without notice, after which this version may no longer be accessible.

Existing work has explored faster sorter architectures [7], [8] and methods that reduce the number of candidates entering the sort [9], [10]. Sort-free variants have also been reported, including partial-expansion approaches [11] and Distributed K-Best (DKB) that rely on iterative selection via multi-way merge networks [12]–[14], with further reductions in iteration count using discretized path-metric search [15]. Even so, these K-Best families still depend on enumeration-based expansion, keeping the overall complexity tied to $|\mathcal{A}|$ [5], [6].

Recently, Box Decoding was proposed as a sort-free tree-search MIMO detector that avoids constellation-wise enumeration [16]. At each layer, it uses quantization to form a fixed-size candidate grid (“box”) around a ZF estimate, enabling complexity independent of the QAM order, while often achieving error performance close to K -Best. The method has mainly been demonstrated for small dimensions (e.g., 2×2 MIMO), since the lack of pruning makes the number of visited nodes grow exponentially with the MIMO order. A related variant, K -Box [17], reduces this growth by reintroducing sorting, but the associated overhead is hardware-unfriendly, especially for parallel architectures.

This letter addresses the scalability bottleneck of Box Decoding. Our contributions are threefold:

- 1) three deterministic, low-complexity, and sort-free pruning strategies—Single-Step Candidate Pruning (SCP), Iterative Candidate Pruning (ICP), and hybrid SICP_m—are proposed to extend Box Decoding beyond the original 2×2 MIMO dimension by suppressing exponential node growth without sorting;
- 2) the pruning rules exploit the geometric symmetry of the QAM grid and the relative position between the ZF estimate and nearby constellation points to reduce node visits and often bypass full Euclidean-distance computations;
- 3) the resulting detector remains QAM-order-independent and sort-free, and its regular comparison-based structure maps naturally to parallel hardware. Simulations confirm substantial complexity savings with negligible BER degradation.

Notations: a , \mathbf{a} , and \mathbf{A} denote a scalar, a vector, and a matrix, respectively. \mathbf{A}^H represents the Hermitian of \mathbf{A} , whereas $|\mathbf{a}|^2$ and $\lfloor \cdot \rfloor$ denote the norm-squared and the floor operation, respectively. Finally, symbols \mathbb{C} , \Re , and \Im denote the complex field, and the real and imaginary parts of a complex number, respectively.

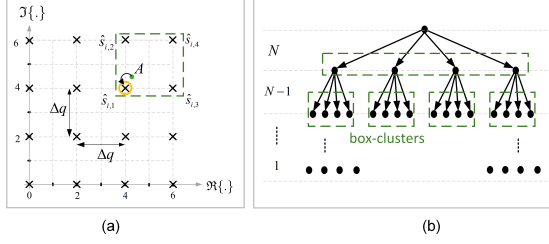


Fig. 1: Box decoding example (reproduced from [16]): (a) Box operation on a 16-QAM map grid (positive quadrant); (b) Box decoder tree structure with box size $\mathcal{B} = 4$.

II. System Model

A. Tree-Based MIMO Detection

Consider a point-to-point $N \times N$ MIMO system [2] with transmitted symbol vector $\mathbf{s} \in \mathcal{A}^N$, received symbol vectors $\mathbf{y} \in \mathcal{A}^N$ and channel $\mathbf{H} \in \mathbb{C}^{N \times N}$. For tree-search detection, apply the QR decomposition $\mathbf{H} = \mathbf{Q}\mathbf{R}$ (unitary \mathbf{Q} , upper-triangular \mathbf{R}) to obtain

$$\mathbf{x} \triangleq \mathbf{Q}^H \mathbf{y} = \mathbf{R}\mathbf{s} + \mathbf{w}, \quad (1)$$

where $\mathbf{w} = \mathbf{Q}^H \tilde{\mathbf{w}}$, an additive white Gaussian noise (AWGN). The search proceeds from layer $i = N$ to $i = 1$ (last to first row of \mathbf{R}). The partial Euclidean distance (PED) recursion is

$$d_i = d_{i+1} + \left\| x_i - \sum_{j=i+1}^N r_{i,j} \hat{s}_j - r_{i,i} \hat{s}_i \right\|^2, \quad (2)$$

with $d_N = \|x_N - r_{N,N} \hat{s}_N\|^2$. This PED is the search metric for sphere decoding, K -Best, and Box Decoding.

B. Box Decoding Algorithm

The Box Decoding algorithm leverages the structure of the QAM constellation and the upper-triangular nature of the channel matrix after QR decomposition [16]. The decoding starts at layer $i = N$ by forming the reference point (also the ZF estimate) $a_N = \frac{x_N}{r_{N,N}}$, denoted by A in Fig. 1(a) (green). This reference is then quantized to the QAM constellation point in the left-bottom corner via $\left\lfloor \frac{x_N}{r_{N,N}} \right\rfloor$, shown in yellow in Fig. 1(a). More generally, for any subsequent layer i further down the tree, the reference point is computed as $a_i = \frac{x_i}{r_{i,i}}$, where $x_i' = x_i - \sum_{j=i+1}^N r_{i,j} \hat{s}_j$ is the interference-canceled signal from the upper layers.

Given a QAM grid with spacing Δq (Fig. 1(a)), Box Decoding then forms a box of size \mathcal{B} around the reference point A (Box operation). The constellation points within this box at layer i constitute the candidate set $\hat{s}_i = \{\hat{s}^{\text{re}}(l), \hat{s}^{\text{im}}(m)\}$, which is generated as

$$\hat{s}^{\text{re}}(l), \hat{s}^{\text{im}}(m) = \left(\left\lfloor \frac{a_i' - v^{\text{re/im}}}{\Delta q} \right\rfloor + \kappa \right) \Delta q, \quad (3)$$

where $\kappa \in \{l, m\}$ with $l, m \in [-\frac{\sqrt{\mathcal{B}}}{2} + 1, \frac{\sqrt{\mathcal{B}}}{2}]$. Additionally, $v^{\text{re/im}} = \sqrt{\mathcal{A}} - 1$ defines the QAM coordinate span, which ranges from $-v^{\text{re/im}}$ to $+v^{\text{re/im}}$.

The decoder traverses down the tree as illustrated in Fig. 1(b), and repeatedly applies the above quantization and box operation from layer $i = N$ to $i = 2$. In this process, each i -th layer leads to a total of \mathcal{B}^{N-i+1} box candidate nodes corresponding to each reference point a_i . At the bottom of the tree ($i = 1$), the decoder outputs the path $\{\hat{s}_N, \hat{s}_{N-1}, \dots, \hat{s}_1\}$ that minimizes the total accumulated distance

$$d = \sum_{i=N}^1 \left| x_i - \sum_{j=i+1}^N r_{i,j} \hat{s}_j \right|^2.$$

To address the limitation of exponentially growing complexity, pruning can be introduced at designated layers. Based on the chosen rule, only a subset of child nodes is retained and expanded further. The proposed pruning strategies are described in detail in Section III.

III. Low-Complexity Box Candidate Pruning

A. Efficient PED Comparison Techniques

As shown in Fig. 1(b), each parent node at layer $i + 1$ generates a fixed set of candidate nodes, referred to as a 'box cluster' at layer i . Since all candidates in a cluster originate from the same parent and differ only in their positions within the QAM grid, we can exploit the regular structure of the QAM grid to derive low-complexity approaches for comparing the PEDs.

1) Local PED Minimum Rule (Metric 1): Assuming a box size of $\mathcal{B} = 4$ at layer i , as illustrated in Fig. 1(a), the PED associated with each node $\hat{s}_{i,b}$ can be derived from (2) as

$$d_{i,b} = d_{i+1} + r_{i,i}^2 \|a_i - \hat{s}_{i,b}\|^2; \quad b = 1, \dots, \mathcal{B}, \quad (4)$$

where d_{i+1} is the accumulated PED from upper layers, and a_i is the reference point at layer i . Since d_{i+1} , a_i and $r_{i,i}$ are identical for all candidates within a box cluster, their PED differences arise solely from the Euclidean distance term. For instance, the PED difference between two candidates $\hat{s}_{i,2}$ and $\hat{s}_{i,1}$ is given by

$$\begin{aligned} d_{i,2} - d_{i,1} &\stackrel{(a)}{=} r_{i,i}^2 (\|a_i - \hat{s}_{i,2}\|^2 - \|a_i - \hat{s}_{i,1}\|^2) \\ &\stackrel{(b)}{=} -r_{i,i}^2 (2\mathcal{I}\{\delta_1\} - \Delta q) \Delta q, \end{aligned} \quad (5)$$

where $\delta_1 = a_i - \hat{s}_{i,1}$. Step (a) follows from the structure of the PED expression, while (b) assumes the two candidates differ only in their imaginary components, i.e., $\mathcal{I}\{\hat{s}_{i,2}\} = \mathcal{I}\{\hat{s}_{i,1}\} + \Delta q$, with identical real components, as illustrated in Fig. 1(a). This leads to the simple comparison rule:

$$\Delta q - 2\mathcal{I}\{\delta_1\} \lesseqgtr 0, \quad (6)$$

which allows us to determine whether $\hat{s}_{i,1}$ or $\hat{s}_{i,2}$ yields a smaller PED without explicitly performing distance calculations. A similar rule applies when comparing candidates

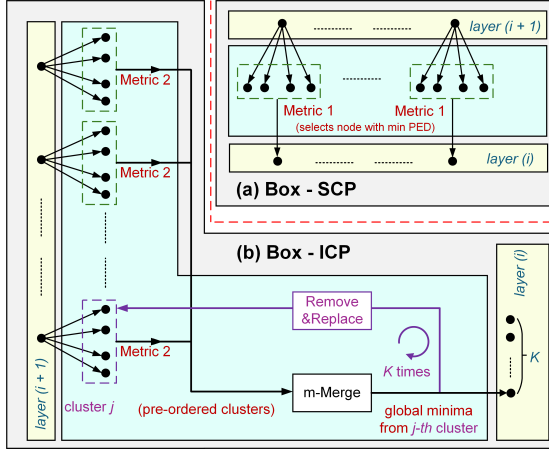


Fig. 2: Block diagram of the proposed box pruning strategies; (a) Box-SCP and (b) Box-ICP with box size $\mathcal{B} = 4$.

that differ along the real axis, leading to the corresponding decision rule:

$$\Delta q - 2\Re\{\delta_1\} \lesseqgtr 0. \quad (7)$$

Due to the geometric symmetry of the QAM constellation, several PED differences among candidates within a box cluster are equal. For example, the PED difference between $\hat{s}_{i,2}$ and $\hat{s}_{i,1}$ is equal to that between $\hat{s}_{i,4}$ and $\hat{s}_{i,3}$; similarly, the difference between $\hat{s}_{i,3}$ and $\hat{s}_{i,1}$ matches that between $\hat{s}_{i,4}$ and $\hat{s}_{i,2}$. These relationships can be expressed as:

$$d_{i,3} - d_{i,1} = d_{i,4} - d_{i,2}; \quad d_{i,2} - d_{i,1} = d_{i,4} - d_{i,3}. \quad (8)$$

This symmetry enables us to identify the best candidate (i.e., the one with the minimum PED increment) within a box cluster using only the simplified comparisons in (6) and (7), collectively referred to as Metric 1.

From a computational cost perspective, the PED comparisons in Metric 1 involve constant left shifts (multiplication by 2), which are typically implemented as hardwired bit-shifts and require negligible logic. Furthermore, the offset $\delta_1 = a_i - \hat{s}_{i,1}$, required in Metric 1, is already computed during the Box Operation step during candidate nodes generation.

2) Local PED Ordering Rule (Metric 2): While Metric 1 identifies only the candidates with the maximum and minimum PED values within a box cluster, additional rules are required to determine the relative ordering of all candidates based on their PEDs. Extending the logic used in (5), the PED differences between $\hat{s}_{i,3}$ and $\hat{s}_{i,2}$, as well as between $\hat{s}_{i,4}$ and $\hat{s}_{i,1}$, lead to the following comparison rules:

$$\begin{aligned} d_{i,3} - d_{i,2} \lesseqgtr 0 &\Rightarrow \Re\{\delta_1\} - \Im\{\delta_1\} \lesseqgtr 0 \\ d_{i,4} - d_{i,1} \lesseqgtr 0 &\Rightarrow \Re\{\delta_1\} + \Im\{\delta_1\} - \Delta q \lesseqgtr 0. \end{aligned} \quad (9)$$

Equations (6), (7) and (9) are collectively referred to as the Metric 2, which determines the order of candidate nodes within a box cluster of size $\mathcal{B} = 4$. For larger box sizes (e.g., $\mathcal{B} = 16, 64$), Metric 2 is typically applied to the four nearest neighboring constellation points around a_i , which is generally sufficient for candidate pruning in most practical systems.

B. Proposed Candidate Pruning Strategies

1) Single-Step Candidate Pruning (SCP): The SCP strategy, as illustrated in Fig. 2(a), selects one candidate node per box cluster at each detection layer using Metric 1. Since candidates within a cluster share the same parent node and differ only in their relative constellation positions, Metric 1 enables efficient local comparisons without explicit PED computation or sorting. This allows a single child node to be chosen per parent, forming the core of the SCP pruning strategy.

While SCP reduces complexity, it does not guarantee that the globally best candidates are retained, as pruning is performed independently across clusters. In particular, some clusters may contain multiple candidates with lower PEDs than those selected in other clusters, a limitation we refer to as the optimal child node skip problem. To address this, we introduce the ICP strategy, which iteratively refines candidate selection across clusters.

2) Iterative Candidate Pruning (ICP): To overcome the limitation of SCP, the ICP strategy adopts the MultiWay Merge (m-Merge) [14] technique to iteratively generate the required child nodes. The m-Merge algorithm efficiently combines several pre-sorted source lists into a single ordered sequence by repeatedly selecting the global minimum from the local minima of all lists and replacing it with the next-best element from the same list. This approach avoids exhaustive candidate evaluations while ensuring that only the most promising nodes are expanded.

In the context of Box Decoding, each box cluster is treated as an individual source list for m-Merge operation. Before merging, candidates in each box cluster are pre-ordered using Metric 2. The local minima from all clusters are then compared to identify the global best candidate, which is removed and replaced by the next element from the same cluster. This process is repeated until K child nodes are selected. As illustrated in Fig. 2(b), ICP is applied at a designated detection layer after the Box Operation has expanded the candidate list. Unlike the DKB algorithm [12], which integrates m-Merge with explicit PED calculations, ICP leverages Metric 2 to maintain QAM-size independence while eliminating unnecessary computations. Moreover, by visiting only the required subset of candidates instead of evaluating all possible nodes at each stage as in conventional K -Best detection, ICP achieves substantial complexity reduction.

3) Hybrid SCP-ICP Candidate Pruning (SICP): The ICP strategy was introduced to overcome the optimal child-node skip problem and guarantee the selection of globally best candidates. However, full ICP across all layers incurs additional iterations that are not always necessary, since accurate pruning in the early layers already leads to substantial performance improvements. To balance complexity and accuracy, we propose a hybrid scheme, termed SCP-ICP (SICP_m), which applies ICP only in the first m layers and reverts to SCP in the remaining layers.

IV. Complexity Analysis

A. Number of Visited Node

At any detection layer i , a candidate node is considered visited once its PED is computed and used in the pruning or sorting stage. Let \mathcal{P}_i denote the number of visited candidate nodes and K_i the number of surviving child nodes passed to the next layer. A larger \mathcal{P}_i implies a greater number of PED calculations and comparisons, whereas K_i determines the complexity of the interference cancellation in the quantization step (Sec. II-B). As will be shown in Sec. V, detectors maintaining a constant K_i at each layer achieve comparable bit error rate (BER) performance. To ensure a fair complexity comparison, we therefore fix $K_i = K$ (a constant) for $i = 1, \dots, N$ across all schemes and report \mathcal{P}_i , which is determined solely by the candidate expansion rule.

In conventional K -Best, each parent enumerates the full constellation \mathcal{A} , giving $\mathcal{P}_i = \mathcal{A}K$. In DKB [12], K nodes are selected for the first child, while an additional $K - 1$ nodes are visited for the remaining child nodes. In the complex-value domain, a further $K - 1$ nodes are visited via complex Schnorr–Euchner (SE) enumeration, yielding $\mathcal{P}_i = 3K - 2$. In the proposed ICP strategy, SE enumeration is replaced by Metric 2 for candidates ordering, reducing the visits to $\mathcal{P}_i = 2K - 1$. For Box-SCP, exactly one candidate per box cluster is evaluated, resulting in $\mathcal{P}_i = \mathcal{B}$. These visit counts directly correspond to the number of PED computations and comparisons required per layer in the pruning or sorting stage.

Table I summarizes the number of visited nodes for 4×4 and 8×8 MIMO with $K = \mathcal{B} = 4$ and different \mathcal{A} . The proposed Box-SCP, Box-ICP and hybrid Box-SICP _{m} visit far fewer nodes than conventional K -Best and DKB. Moreover, their visit counts are independent of \mathcal{A} and determined solely by the tunable box size \mathcal{B} , enabling a clear performance–complexity trade-off. For example, Box-ICP requires 22 and 50 visits, while Box-SCP needs only 16 and 32 for 4×4 and 8×8 , respectively. The hybrid Box-SICP _{m} achieves intermediate complexity, with 19 visits for 4×4 ($m = 1$) and 35 to 41 nodes for 8×8 with $m = 1 - 3$. Compared to DKB, these totals correspond to reductions of 37.5% (Box-ICP), 48.8–56.3% (Box-SICP _{m}), and 60% (Box-SCP). Since each visit maps directly to a PED computation, these savings translate into proportional reductions in arithmetic and hardware cost.

B. Complexity in Hardware Implementation

Although DKB’s visit count is independent of \mathcal{A} (Table I), its hardware cost still scales with \mathcal{A} as selecting the first child still requires comparisons against a central-value set C of size $C = \sqrt{\mathcal{A}}$ [6]. For example, for 64-QAM, $C = \{\pm R_{ii}, \pm 3R_{ii}, \pm 5R_{ii}, \pm 7R_{ii}\}$. Constructing this set requires extra multipliers for $\times R_{ii}$ (even if implemented by shift–add), registers to store the values in C , and comparators for selection, all of which grow with $|C|$ and become significant for higher-order QAM. In contrast, the

TABLE I: The number of visited node of proposed Box-SCP, Box-ICP, Box-SICP _{m} , K -Best and DKB with $K = \mathcal{B} = 4$.

Decoding Algorithm	Equation	4×4 MIMO	8×8 MIMO		
K -Best	$\mathcal{A} + \mathcal{A}K(N - 1)$	52/208/832 ⁽²⁾	100/464/1856 ⁽²⁾		
DKB ⁽¹⁾	$(3K - 2)N$	40	80		
Box	\mathcal{B}^N	256	4 ⁸		
Box-SCP	$N\mathcal{B}$	16	32		
Box-ICP	$2\mathcal{B} + (2K - 1)(N - 2)$	22	50		
Box-SICP _{m}	$2\mathcal{B} + m(K - 1) + (N - 2)K$	$m = 1$	$m = 1$	$m = 2$	$m = 3$
		19	35	38	41

⁽¹⁾DKB in complex mode

⁽²⁾for 4/16/64-QAM

proposed strategies avoid this overhead by using Metric 1 to locate the nearest point with only two comparators, and Metric 2 to order the four closest points with just five comparators. This eliminates the need to explore or register the full QAM map, yielding a truly QAM-independent, sort-free candidate selection mechanism.

Additionally, Box-SCP enables layer-wise, fully parallel processing. Unlike sorting in conventional K -Best, or the m-Merge in DKB, Box-SCP uses Metric 1 to select the local minimum within each box cluster independently. Since no global ordering or merging is required, all clusters can be processed concurrently and surviving child nodes are obtained in a single step. This order-free candidate selection shortens the critical path and makes Box-SCP particularly well suited for low-latency hardware implementations. However, due to the optimal child-node skip problem, Box-SCP incurs a modest BER loss relative to Box and K -Best. For BER-critical scenarios, Box-ICP and hybrid Box-SICP _{m} mitigate this by applying m-Merge in the pruning layers at the expense of reduced parallelism.

V. Simulation Results

A. BER performance analysis

This section presents the BER performance of the proposed Box-SCP, Box-ICP, and hybrid Box-SICP _{m} schemes, benchmarked against linear ZF, LMMSE, the optimal ML detector, conventional K -Best, and Box Decoding without pruning. Note that (i) DKB differs from K -Best only in candidate expansion and selection schemes, with identical BER for the same K , and is therefore omitted from the plots; and (ii) as with other state-of-the-art K -Best variants, none can outperform conventional K -Best under identical K , making it the baseline.

All simulations are performed over an i.i.d. Rayleigh flat-fading MIMO channel with perfect channel state information (CSI) at the receiver. For fairness, the number of surviving nodes per layer is fixed at $K = \mathcal{B} = 4$ for all schemes, similar to [16]. Performance is compared at BER = 10^{-3} for 4-QAM and 16-QAM, which is standard for uncoded systems. For 64-QAM, neither K -Best nor the original Box Decoding without pruning reach BER = 10^{-3} even beyond 30 dB SNR; therefore, results at 25 dB SNR are reported for comparison.

Fig. 3a shows BER for 4×4 MIMO with 4-QAM, 16-QAM and 64-QAM. At 4-QAM Box attains ML performance since $\mathcal{A} = \mathcal{B}$ and all constellation points are evaluated within one box. For higher-order QAM, Box is

no longer optimal ($\mathcal{B} < \mathcal{A}$) but closely follows K -Best. The effect of pruning on Box is modest: Box-ICP tracks K -Best and Box (without pruning) across all QAM configurations, while Box-SCP incurs SNR losses of roughly 3 dB, 1 dB, 0.7 dB for 4-QAM, 16-QAM and 64-QAM, respectively. Introducing one iterative pruning layer into the Box-SCP (Box-SICP₁) largely closes this gap, approaching K -Best with only a negligible residual loss.

Similarly, Fig. 3b shows BER for 8×8 MIMO, where all Box variants (both with and without pruning) follow the same trend in Fig. 3a. Box Decoding coincides with ML at 4-QAM and tracks K -Best at 16/64-QAM, while Box-ICP follows K -Best with an SNR loss of about 2.5 dB at 4-QAM, deviating away from the ML-like slope. This loss arises due to the exponentially large hypothesis space ($4^8 = 65,536$ for 8×8 , 4-QAM) and the fixed small set of surviving nodes ($K = 4$), which can cause the true ML path to be pruned early, leading to pruning-limited rather than noise-limited errors. Furthermore, Box-SCP shows larger degradation than in 4×4 , with losses of about 5 dB, 2 dB and 1.3 dB for 4-QAM, 16-QAM and 64-QAM, respectively. However, introducing ICP layers in Box-SCP alleviates this: Box-SICP₁ improves performance by about 3.5 dB, 1.2 dB and 0.7 dB for the three constellations, yielding curves close to K -Best.

B. Performance and Complexity Trade-off

The BER-complexity trade-offs can be summarized as follows:

- 1) With $K = \mathcal{B}$ the proposed sort-free pruning strategies (SCP, ICP, and hybrid SICP_{*m*}) achieve near- K -Best BER and a ≥ 5 dB SNR gain over ZF/MMSE while reducing the visited-node count by 33-66% relative to DKB. From a hardware perspective, they also avoid QAM-dependent operations and registers, supporting scalability to larger constellations.
- 2) The hybrid detection scheme Box-SICP_{*m*} provides a tunable BER-complexity trade-off by adjusting the number of ICP layers ($1 \leq m \leq N - 2$). A single ICP layer ($m = 1$) is typically sufficient to achieve near- K -Best performance for $\mathcal{A} \geq \mathcal{B}$ with ≤ 0.5 dB performance loss and complexity close to Box-SCP, while additional ICP layers ($m > 1$ or Box-ICP) bring negligible benefit.
- 3) Box-SCP removes sorting/SE enumeration entirely, enabling fully parallel, layer-wise tree search with maximal complexity savings. Its BER penalty relative to K -Best is modest and diminishes with increasing constellation size, making it well suited to vectorized implementations with very high-order constellations ($\mathcal{A} \gg \mathcal{B}$).

VI. Conclusions

In this paper, we proposed low-complexity, sort-free candidate pruning strategies, viz., SCP, ICP and hybrid SICP_{*m*} to address the exponential complexity growth of

Box Decoding for large-scale MIMO detection. By exploiting the geometric regularity of the QAM grid, the proposed methods enable candidate selection without traversing the entire constellation map. Combined with Box Decoding, these pruning schemes eliminate sorting and QAM-dependent operations, making them highly suited for hardware-efficient implementation. Simulation results demonstrated that the proposed detectors achieve near- K -Best performance with substantial reductions in visited nodes and computational cost. These advantages establish Box Decoding with pruning as a scalable and modulation-independent solution for high-throughput MIMO systems. Future work will focus on hardware implementation and evaluating the proposed schemes under practical channel conditions.

References

- [1] S. Yang and L. Hanzo, "Fifty Years of MIMO Detection: The Road to Large-Scale MIMOs," *IEEE Commun. Surveys & Tutorials*, vol. 17, no. 4, pp. 1941–1988, 2015.
- [2] E. Larsson, "MIMO Detection Methods: How They Work [Lecture Notes]," *IEEE Signal Process. Magazine*, vol. 26, no. 3, pp. 91–95, 2009.
- [3] E. Viterbo and J. Boutros, "A Universal Lattice Code Decoder for Fading Channels," *IEEE Trans. on Information Theory*, vol. 45, no. 5, pp. 1639–1642, 1999.
- [4] Z. Guo and P. Nilsson, "Algorithm and Implementation of the K-Best Sphere Decoding for MIMO Detection," *IEEE Journal on Selected Areas in Commun.*, vol. 24, no. 3, pp. 491–503, 2006.
- [5] S. Mondal, A. Eltawil, C.-A. Shen, and K. N. Salama, "Design and Implementation of a Sort-Free K-Best Sphere Decoder," *IEEE Trans. on Very Large Scale Integr. (VLSI) Sys.*, vol. 18, no. 10, pp. 1497–1501, 2010.
- [6] M.-T. Shiue, S.-S. Long, C.-K. Jao, and S.-K. Lin, "Design and Implementation of Power-Efficient K-Best MIMO Detector for Configurable Antennas," *IEEE Trans. on Very Large Scale Integr. (VLSI) Syst.*, vol. 22, no. 11, pp. 2418–2422, 2014.
- [7] B. Y. Kong and I.-C. Park, "Improved sorting architecture for K-best mimo detection," *IEEE Trans. on Circuits and Syst. II: Express Briefs*, vol. 64, no. 9, pp. 1042–1046, 2017.
- [8] Y.-R. Chen, C.-C. Ho, W.-T. Chen, and P.-Y. Chen, "A low-cost pipelined architecture based on a hybrid sorting algorithm," *IEEE Trans. on Circuits and Syst. I: Regular Papers*, vol. 71, no. 2, pp. 717–730, 2024.
- [9] Y. Tian, W. Bian, J. Zheng, W. Zhou, Y. Huang, and C. Zhang, "Breadth-first search detection with permutation channel for massive mimo," *IEEE Wireless Commun. Letters*, pp. 1–1, 2025.
- [10] J. Zheng, Y. Sun, H. Zhou, W. Zhou, Y. Huang, X. You, and C. Zhang, "Low-complexity breadth-first search detection for large-scale mimo syst," *IEEE Trans. on Commun.*, vol. 73, no. 8, pp. 5667–5681, 2025.
- [11] K. Amiri, C. Dick, R. Rao, and J. R. Cavallaro, "Novel sort-free detector with modified real-valued decomposition (m-rvd) ordering in mimo syst." in *IEEE GLOBECOM 2008 - 2008 IEEE Global Telecommun. Conference*, Nov 2008, pp. 1–5.
- [12] M. Shabany, K. Su, and P. Glenn Gulak, "A Pipelined Scalable High-Throughput Implementation of a Near-ML K-Best Complex Lattice Decoder," in *2008 IEEE International Conference on Acoustics, Speech and Signal Processing*, 2008, pp. 3173–3176.
- [13] M. Shabany and P. G. Gulak, "The Application of Lattice-Reduction to the K-Best Algorithm for Near-Optimal MIMO Detection," in *Proc. IEEE Int. Symp. on Circuits and Syst. (ISCAS)*, 2008, pp. 316–319.
- [14] D.-L. Lee and K. Batcher, "A Multiway Merge Sorting Network," *IEEE Trans. on Parallel and Distrib. Syst.*, vol. 6, no. 2, pp. 211–215, 1995.
- [15] Y.-X. Liu, S.-J. Jihang, and Y.-L. Ueng, "An efficient k-best mimo detector for large modulation constellations," *IEEE Open Journal of Circuits and Syst.*, vol. 5, pp. 2–16, 2024.

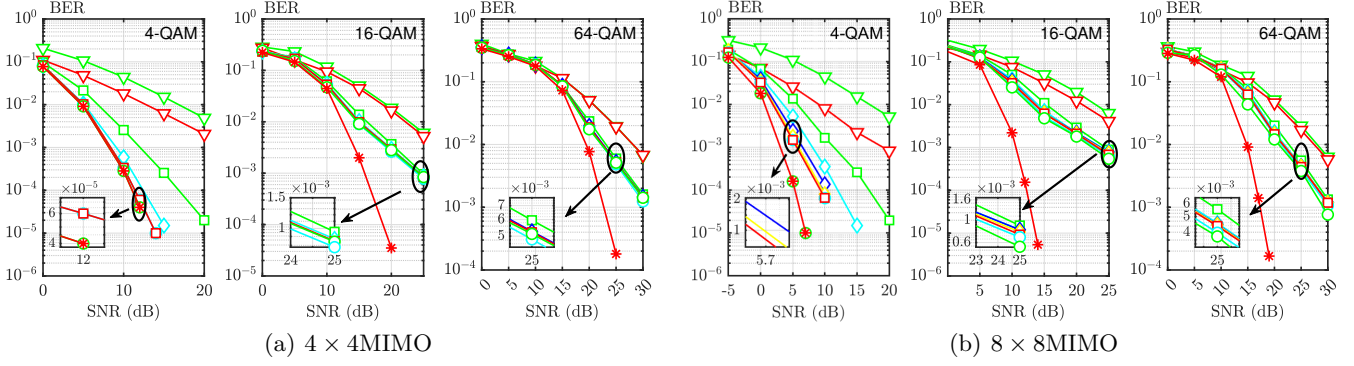


Fig. 3: BER performance of detection schemes ($\text{--}\nabla\text{--}$: ZF; $\text{--}\nabla\text{--}$: LMMSE; $\text{--}\square\text{--}$: Box-SCP; $\text{--}\diamond\text{--}$: Box-SICP₁; $\text{--}\diamond\text{--}$: Box-SICP₂; $\text{--}\diamond\text{--}$: Box-SICP₃; $\text{--}\circ\text{--}$: K -Best; $\text{--}\square\text{--}$: Box-ICP; $\text{--}\circ\text{--}$: Box; $\text{--}\ast\text{--}$: ML for 4-QAM or SD for 16/64-QAM).

- [16] S. F. Qureshi, S. A. Damjanecvic, E. Matus, D. Utyansky, P. Van Der Wolf, and G. P. Fettweis, "Box Decoding: A Low-Complexity Algorithm for MIMO Detection," in 2024 IEEE Workshop on Signal Processing Syst. (SiPS), 2024, pp. 25–30.
- [17] H. Zhang, S. F. Qureshi, E. Matuš, D. Utyansky, P. Van der Wolf, and G. P. Fettweis, "A Low-Complexity K-Box Detector in High-Dimensional MIMO Systems," in Proc. IEEE 102nd Veh. Technol. Conf., Oct 2025, (to appear).